“free” excitons to the Xe impurity.

---

*Work supported by the National Council for Research and Development, Israel.

[1] J. Jortner, L. Meyer, S. A. Rice, and E. G. Wilson, J. Chem. Phys. 42, 4250 (1965).

[2] A. Gedanken, B. Raz, and J. Jortner, J. Chem. Phys. 58, 1178 (1973).

[3] O. Cheshnovsky, B. Raz, and J. Jortner, J. Chem. Phys. 59, 3301 (1973).

[4] B. Raz and J. Jortner, Proc. Roy. Soc., Ser. A 317, 113 (1970).

[5] L. Apker and E. Taft, Phys. Rev. 79, 964 (1950), and 81, 698 (1951).

[6] M. Martin, J. Chem. Phys. 54, 3289 (1971).

[7] Gedanken, Raz, and Jortner, Ref. 2.

[8] G. Baldini, Phys. Rev. 128, 1562 (1962).

[9] G. Baldini, Phys. Rev. 137, A508 (1965).

[10] Z. Ophir, U. Even, B. Raz, and J. Jortner, “Pulsed High Pressure Lamp for the Vacuum Ultraviolet” (to be published).

[11] The photon current was normalized to the total photon flux hitting the sample. A small (10%) correction due to reflection of the pure matrix was neglected.

[12] J. F. O'Brien and K. J. Teegarden, Phys. Rev. Lett. 17, 919 (1966).

[13] N. Schwentner, M. Skibowski, and W. Steinmann, to be published.

[14] S. I. Choi and S. A. Rice, J. Chem. Phys. 38, 366 (1963).

[15] This estimate is based upon taking the absolute value $Y = 13\%$ for solid Xe at 10.3 eV, obtained by Schwentner (private communication).

[16] M. Hebb, Phys. Rev. 81, 702 (1951).

[17] O. Simpson, Proc. Roy. Soc., Ser. A 238, 402 (1957).

[18] P. Avakian, V. Ern, R. E. Merrifield, and A. Suna, Phys. Rev. 165, 974 (1968).

[19] Y. Toyozawa, Progr. Theor. Phys. 20, 53 (1958).

[20] A. Gold and R. S. Knox, J. Chem. Phys. 36, 2805 (1962).

[21] S. D. Druger, J. Chem. Phys. 54, 2339 (1971).

Temperature Dependence of Conductivity of Tetrathiafulvalene-Tetracyanoquinodimethane (TTF-TCNQ) Single Crystals

R. P. Groff, A. Suna, and R. E. Merrifield
Central Research Department, E. I. du Pont de Nemours and Company, Wilmington, Delaware 19898

(Received 22 May 1974)

The conductivity of single crystals of tetrathiafulvalene-tetracyanoquinodimethane (TTF-TCNQ) was measured over the temperature range 40–300 K. The maximum low-temperature conductivity parallel to the *b* axis ranged from 12–35 times the corresponding room-temperature value. The temperature dependence of the intrinsic conductivity (after residual resistivities were excluded) was the same for all crystals measured and was fitted by a $T^{-2.33 \pm 0.14}$ dependence for $60 \leq T \leq 300$ K.

Extraordinary maxima[1] in the apparent electrical conductivity of single crystals of tetrathiafulvalene-tetracyanoquinodimethane (TTF-TCNQ) have alternately been ascribed to the presence of superconducting fluctuations[1] or experimental artifacts.[2] There is considerable disagreement on the experimental results for the conductivity obtained in different laboratories.[3,4] We have measured the conductivity along the *a* and *b* axes of a number of TTF-TCNQ single crystals. Our measurements show that the temperature dependence of the *b*-axis conductivity of TTF-TCNQ can be described by a single function, even for crystals whose conductivity enhancement differs by a factor of 3.

Solution-grown TTF-TCNQ crystals were prepared under argon, at room temperature, in acetonitrile, by diffusion of $5 \times 10^{-3} M$ solutions of the two components into an equal volume of pure solvent. Both the TTF and TCNQ had been twice gradient sublimed under argon. Crystal growth was allowed to proceed for five days before harvesting. These crystals grow preferentially along the *b* axis with a laminar structure in which individual laminae are oriented parallel to the *a*-*b* plane. In order best to deal with the problem of nonuniform conductivity between laminae for *b*-axis measurements, crystals were selected with one perfectly developed *a*-*b* face and as free as possible from defects, inclusions, etc., visible in transmission microscopy with collimated incident light. Conventional dc measurement techniques were adopted with four silver-paste (Du Pont No. 7941 thinned with octyl acetate or hexyl acetate) electrodes attached to the best developed *a*-*b* face. This arrangement gave more reproducible results than such alternative electrode configurations as wrapping the

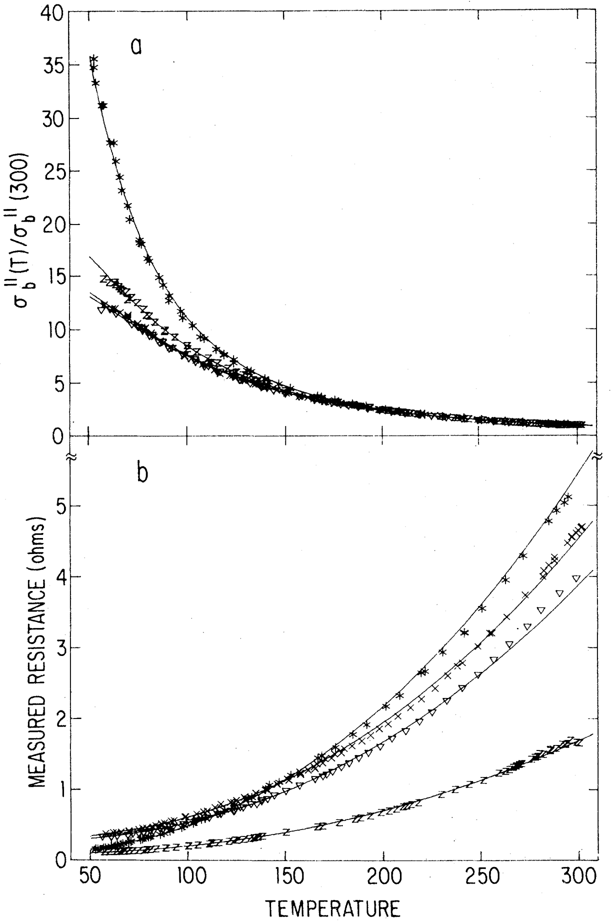

FIG. 1. (a) Normalized conductivity measured parallel to the b axis for four TTF-TCNQ crystals. (b) Measured resistance versus temperature for the same crystals. (Vertical scale expanded 10 × for the crosses). Solid curves in both parts of the figure are fits by $\rho = \rho_0 + AT^{2.33}$.

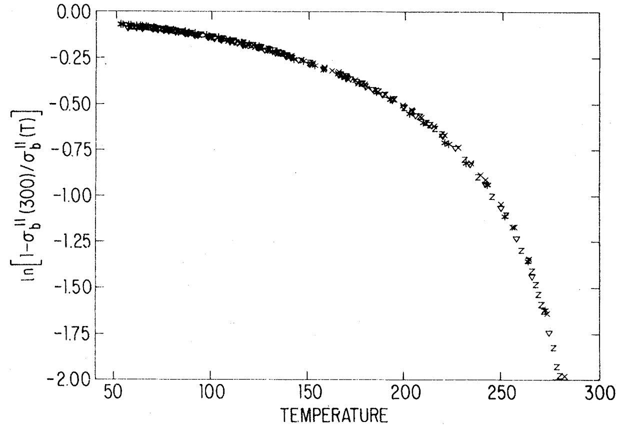

FIG. 2. Plot of $\ln[1-\sigma_b^{\parallel}(300)/\sigma_b^{\parallel}(T)]$ versus temperature for the four crystals in Fig. 1 (see text for explanation).

electrodes around the crystals. Crystals with resistances not reproducing to better than 2% upon warming and cooling the sample were discarded. Room-temperature conductivities[5] along the b axis ($\sigma_b^{\parallel}$) typically ranged from 250–500 $(\Omega\ \mathrm{cm})^{-1}$.

All conductivity measurements along the a axis ($\sigma_a^{\parallel}$) were made on single crystals grown from the vapor which grew preferentially along the a axis. These crystals were prepared in sealed Pyrex ampules under 1–10 Torr He at ca. 400 K. Room-temperature conductivities were typically 1 $(\Omega\ \mathrm{cm})^{-1}$, increasing to ca. 2.2 $(\Omega\ \mathrm{cm})^{-1}$ at the transition.[6]

Figure 1(a) shows a plot of the conductivity $\sigma_b^{\parallel}$ versus temperature for four crystals with low-temperature maxima ranging from 12 to 35 times the corresponding values at 300 K. Although we show only data above the apparent transition, none of the samples shown here exhibited any traces of the "double maximum" reported in Ref. 4. Figure 1(b) shows the same data plotted as resistances.

If we suppose that we can separate the sample resistivity $\rho(T)$ into a sample-dependent residual component ρ_0 and some unknown function $f(T)$ which describes the intrinsic temperature dependence of the material, i.e.,

$$\rho(T) = \rho_0 + f(T), \tag{1}$$

we can write

$$\ln\left(1-\frac{\rho(T)}{\rho(T_1)}\right) = \ln\left(1-\frac{f(T)}{f(T_1)}\right) - \ln\left(1+\frac{\rho_0}{f(T_1)}\right), \tag{2}$$

where T_1 is some conveniently chosen normalization temperature. The important feature here is that properties having to do with a given crystal appear in the second term on the right-hand side while the first term contains only the intrinsic temperature dependence of the material. Hence a plot of $\ln[1-\sigma(T_1)/\sigma(T)]$ versus T should yield a series of identical curves displaced parallel to one another along the vertical direction. (A simple plot of ρ versus T would also have this feature; however, it is not possible to determine absolute values of ρ accurately.[5]) Figure 2 shows such a plot using data shown in Fig. 1 and choosing $T_1 = 300$ K. The curves have been displaced vertically to make comparison easier.[7]

The bottom curve of Fig. 3 shows typical results of conductivity $\sigma_a^{\parallel}(T)$ plotted in a similar fashion. For comparison the points in the middle

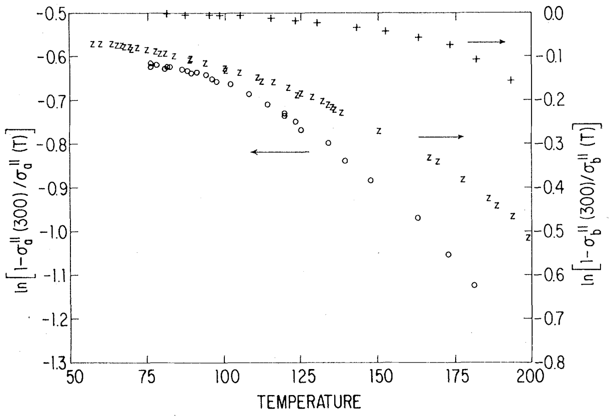

FIG. 3. Comparison of functional forms of (bottom curve) conductivity parallel to the *a* axis, (middle curve) conductivity parallel to the *b* axis, and (top curve) intentionally generated "false" conductivity data of Ref. 2.

curve show a sample from Fig. 1 with a low-temperature conductivity maximum ca. 12 times its room-temperature value. The different functional forms are clearly evident. The top curve shows the intentionally generated "false" conductivity data of Ref. 2 plotted in this fashion.

The method outlined above provides a sensitive test for making quantitative comparisons between theory and experiment. For example, it has been suggested[4,8] that

$$f(T)=AT\exp(B/T). \tag{3}$$

However, a plot such as shown in Figs. 2 and 3 demonstrates dramatically that Eq. (3) does not fit the available data (with $T_1=300$ K), although a limited region can be fitted if T_1 is chosen to be below 200 K (cf. Ref. 4).

We have found that a remarkably good fit (2% standard deviation) to all our data, over the temperature range 60 to 300 K, can be obtained with

$$f(T)/f(T_1)=(T/T_1)^{\lambda} \tag{4}$$

where $\lambda=2.33$. The solid curves of Fig. 1 have been obtained from Eqs. (1) and (4), by least-squares adjustment of ρ_0 and the normalization of $f(T)$. The mean square *relative* deviation[9] has been minimized, so that an equally good fit appears in plots of the conductivity [Fig. 1(a)] and of the resistance [Fig. 1(b)]. Somewhat improved fits can be obtained by optimizing λ for each crystal separately. The resulting values of λ were 2.23, 2.35, 2.36, and 2.40 for the crystals in Fig. 1, with normalized conductivity maxima of 35, 12.5, 12, and 15, respectively. In each case the standard deviation in the value of λ was about 0.14.

The original data of Ferraris *et al.*[3] on less highly purified samples were fitted by a $\lambda=2$ power law for $T \gtrsim 120$ K. This is not inconsistent with $\lambda=2.3$ in view of their experimental uncertainties and lack of reproducibility upon heating and cooling.

A power-law behavior of the conductivity has been calculated by Luther and Peschel[10] in the Tomonaga model of a one-dimensional metal. It is also implied in the second-order renormalization-theory calculations of Sólyom.[11] In a theory similar to that of Luther and Peschel, Mattis[12] finds

$$\sigma(T)=\sigma_0[T/(T+\theta)]^{g}. \tag{5}$$

Our data are fitted by this form only in the limit of infinite θ, although a fit with $\theta \sim E_F/k_B \sim 3000$ K, $g \sim -2.5$ cannot be ruled out. Although Mattis's result was evaluated only for $|g| \ll 1$, no such restriction on the temperature exponent seems to be present in Ref. 10, while Sólyom[11] argues that this exponent should be a universal number, independent of the electron-electron coupling.[13] The power law, Eq. (4), with $\lambda=2.33$, is furthermore consistent with a prediction of Cohen *et al.*[14] that resistivity in a one-dimensional system subject to dynamic disorder should vary as T^2 times a slowly varying function of T.

We also attempted to fit $f(T)$ by the form $(T-T_c)^{\lambda}$, with both T_c and λ variable, but found that only negative values of T_c could improve the fit over the obtained via Eq. (4), and then only slightly. The fact that $f(T)$ thus seems to depend only on T, and not on $T-T_c$, $T_c \sim 58$ K, strongly suggests that the rise in conductivity above the metal-insulator transition near 58 K is not related to this transition but rather is an intrinsic rise which is interrupted by the transition (as, for example, suggested in Ref. 8 and by Lee, Rice, and Anderson[15]).

By setting $\rho_0=0$, we find the maximum expected conductivity enhancement at 58 K: For $\lambda=2.47$, the largest value consistent with our measurements, we have $\sigma(58)/\sigma(300)_{\max}=58$, a result which contradicts greater values reported by workers at the University of Pennsylvania.[1,4]

We wish to thank L. R. Melby and G. J. Sloan for providing the crystals used in this study and P. C. Hoell for use of a computer program.

---

[1] L. B. Coleman, M. J. Cohen, D. J. Sandman, F. G. Yamagishi, A. F. Garito, and A. J. Heeger, Solid State

Commun. 12, 1125 (1973).

[2] D. E. Schafer, F. Wudl, G. A. Thomas, J. P. Ferraris, and D. O. Cowan, Solid State Commun. 14, 347 (1974).

[3] J. P. Farraris, D. O. Cowan, V. Walatka, Jr., and J. H. Perlstein, J. Amer. Chem. Soc. 95, 948 (1973).

[4] M. J. Cohen, L. B. Coleman, A. F. Garito, and A. J. Heeger, Phys. Rev. B (to be published).

[5] Because of uncertainties in where the electrodes actually make contact, these values could be at least a factor of 2 in error. Nevertheless, relative conductivities can be measured with great precision.

[6] Measurements of $\sigma_a^{\parallel}$ tended to be exceptionally reproducible. This is quite unlike the case with $\sigma_b^{\parallel}$ where many crystals had to be discarded to obtain measurements reproducible to ±2%.

[7] The shape of curves such as those shown in Fig. 2 is extremely sensitive to the values of T_1 and $\sigma(T_1)$; hence, reproducible measurements are essential.

[8] P. W. Anderson, P. A. Lee, and M. Saitoh, Solid State Commun. 13, 595 (1973).

[9] Residual $= |R_{\mathrm{meas}} - R_{\mathrm{calc}}|/R_{\mathrm{calc}}$.

[10] A. Luther and I. Peschel, Phys. Rev. Lett. 32, 992 (1974).

[11] J. Sólyom, J. Low. Temp. Phys. 12, 547 (1973).

[12] D. C. Mattis, Phys. Rev. Lett. 32, 714 (1974).

[13] The relation between Sólyom's results and those of the Tomonaga model, Refs. 10 and 12, is discussed by H. Fukuyama, T. M. Rice, and C. M. Varma, Phys. Rev. Lett. 33, 305 (1974); they contend, however, that the sign of the exponent in Sólyom's theory (where conductivity is not explicitly evaluated) would in most cases be such as to give a decreasing conductivity with decreasing temperature.

[14] M. H. Cohen, J. A. Hertz, P. M. Horn, V. K. S. Shante, to be published.

[15] P. A. Lee, T. M. Rice, P. W. Anderson, Phys. Rev. Lett. 31, 462 (1973).

Hyperfine Studies of Site Occupation in Ternary Systems

T. J. Burch* and T. Litrenta
Fordham University,† Bronx, New York 10458

and

J. I. Budnick‡
University of Connecticut, Storrs, Connecticut 06268

(Received 4 June 1974)

The analysis of spin-echo spectra of V, Mn, Co, Ru, Rh, Os, and Ir in Fe_3Si shows that these impurities unexpectedly enter one of the two available Fe sites in a selective manner. Those impurities to the left of Fe in the periodic table prefer the Fe site with eight first-neighbor Fe atoms. Those beneath and to the right of Fe in the periodic table enter the Fe site with four Fe and four Si first neighbors.

From a pulsed NMR study of dilute transition-metal impurities in Fe_3Si and slightly iron-rich off-stoichiometric Fe_3Si, we report an unexpected selective site occupation. Fe_3Si exhibits long-range crystallographic order with a bcc structure and therefore two inequivalent iron sites. In Fig. 1 an element of the Fe_3Si structure is shown. Table I gives the near-neighbor configurations for both Fe and Si out to the third neighbor. Fe_3Si

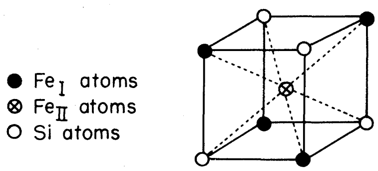

FIG. 1. An element of the Fe_3Si structure showing the Fe_I, Fe_{II}, and Si sites. One Fe site, Fe_I, is on the cube edge and has eight Fe first neighbors; the other Fe site, Fe_{II}, is at the body center and has four Fe and four Si first neighbors; Si is on a cube edge with eight first neighbors.

TABLE I. The first-, second-, and third-nearest-neighbor (nn) configurations for both the Fe and Si sites in Fe_3Si. We specify whether the Fe neighbors are in Fe_I or Fe_{II} sites. If the alloy is slightly Fe-rich, the extra Fe atoms occupy Si sites randomly, producing Fe_{II} sites with not only four but also five, six, and seven Fe first neighbors.

	1 nn	2 nn	3 nn
Fe_{II}	4 Fe_I 4 Si	6 Fe_{II}	12 Fe_{II}
Fe_I	8 Fe_{II}	6 Si	12 Fe_I
Si	8 Fe_{II}	6 Fe_I	12 Si